Geophysical Research Letters

RESEARCH LETTER
10.1029/2022GL098422

A Semi-Empirical Approach for Tsunami Inundation: An Application to the Coasts of South Italy

Lorenzo Melito[1], Francesco Lalli[2], Matteo Postacchini[1], and Maurizio Brocchini[1]

[1]Department of Civil Engineering and Architecture (DICEA), Università Politecnica delle Marche, Ancona, Italy, [2]Italian Institute for Environmental Protection and Research (ISPRA), Rome, Italy

Key Points:

- A modeling chain approach for the evaluation of tsunami inundation is described and applied to the coasts of South Italy
- The method exploits a semi-empirical extension of the classical Green's law to general bathymetries, and dedicated numerical simulations
- The method allows for transposing computational effort from intermediate to shallow waters

Correspondence to:
L. Melito,
l.melito@univpm.it

Citation:
Melito, L., Lalli, F., Postacchini, M., & Brocchini, M. (2022). A semi-empirical approach for tsunami inundation: An application to the coasts of South Italy. *Geophysical Research Letters*, *49*, e2022GL098422. https://doi.org/10.1029/2022GL098422

Received 28 FEB 2022
Accepted 26 MAY 2022

Author Contributions:
Conceptualization: Lorenzo Melito, Francesco Lalli, Matteo Postacchini, Maurizio Brocchini
Data curation: Lorenzo Melito
Formal analysis: Lorenzo Melito, Francesco Lalli
Funding acquisition: Francesco Lalli, Maurizio Brocchini
Investigation: Lorenzo Melito, Francesco Lalli, Matteo Postacchini, Maurizio Brocchini
Methodology: Lorenzo Melito, Francesco Lalli, Matteo Postacchini, Maurizio Brocchini
Project Administration: Francesco Lalli, Maurizio Brocchini
Resources: Francesco Lalli
Software: Lorenzo Melito, Francesco Lalli

Abstract Tsunamis in the Mediterranean Sea have been increasingly investigated recently due to past destructive events. We present a novel operational approach for evaluating tsunami-induced inundation, based on a generalization of Green's law and a chain of intermediate and small-scale simulations. At the intermediate level, simulations with a linear solver are made to identify the distribution of a novel parameter, namely α, condensing all nearshore wave transformations other than shoaling. α represents a proxy for coastal susceptibility to the tsunami impact. Small-scale modeling of coastal flooding performed at locations for which a DTM is freely available, at the Esaro river estuary (Calabria) and in Bari (Apulia), yields inundation levels that compare well with those obtained via intermediate-scale modeling, with a saving in computational time of about 41%. This demonstrates the value of α to "scale" the offshore wave input and reduce computational effort to evaluate flooding at regional scale.

Plain Language Summary An interest in studying the consequences of tsunamis has arisen also for the Mediterranean Sea in the last decades. In this manuscript we present a method for the evaluation of potential coastal inundation caused by the impact of tsunamis. The method exploits a chain of numerical simulations of wave propagation to move the tsunami from the source region down to the investigated coasts. The inundation estimate makes use of a simple parameter, named α, devised to encapsule all the transformation processes the tsunami undergoes in its travel from intermediate waters to the coastline. We apply the method to portions of the southern Italian coast with a prototype tsunami event, and we see that inundation levels achieved with faster, small-scale simulations compare well with those obtained with longer, intermediate-scale simulations. The method can be helpful as an implementation in recent tsunami warning systems developed to warn coastal communities on impending threats.

1. Introduction

The Mediterranean Sea has been subjected since millennia to the action of tsunamis (Ambraseys & Synolakis, 2010; Maramai et al., 2014), yet research interest has seen a boost only recently, in the aftermath of catastrophic events like the Indian Ocean, 2004 (Lay et al., 2005) and Tohoku, 2011 (Mori et al., 2011) tsunamis. The high level of seismic activity characterizing the Mediterranean basin and the ubiquity of coastal communities thriving along its coasts spark the need for studies devoted to characterize tsunami propagation within the Mediterranean Sea and, ultimately, their impact on coastal vulnerability. However, recent applications of vulnerability and risk assessments usually take into account important hydrodynamic variables, for example, sea-level rise, wave height, tide range (Bonaldo et al., 2019; Da Lio & Tosi, 2019; Hzami et al., 2021), but disregard the potential contribution of tsunamis (Anfuso et al., 2021; Chaib et al., 2020).

The potential coastal risk induced by a tsunami wave is function of its energy, which depends on the processes the tsunami experiences while it approaches the coast, for example, shoaling, refraction, diffraction. Since tsunami waves of similar intensity may present significantly different features when propagating over different bathymetries (Madsen et al., 2008; Satake, 1988), tsunami-seabed interaction is fundamental for a proper modeling of long wave evolution and impact. This consideration has sparked our search for an unified modeling approach to effectively consider bathymetry-related processes in tsunami modeling, while conserving general applicability, scientific soundness and ease of execution.

This work presents a methodology to model and predict tsunami-induced coastal inundation. At the core of this methodology is a semi-analytical approach, which combines theoretical grounds and nearshore hydrodynamic modeling to encase the effects of all tsunami transformations into a single, easily understandable parameter.

Supervision: Francesco Lalli, Matteo Postacchini, Maurizio Brocchini
Validation: Lorenzo Melito, Francesco Lalli, Matteo Postacchini, Maurizio Brocchini
Visualization: Lorenzo Melito
Writing – original draft: Lorenzo Melito, Matteo Postacchini
Writing – review & editing: Lorenzo Melito, Francesco Lalli, Matteo Postacchini, Maurizio Brocchini

Similarly, a two-step approach obtained by combining 2D simulations (up to 5–10 m depth) and analytical theory (up to the coast) has been implemented to estimate tsunami runup heights (Choi et al., 2011). Additionally, specific analytical formulations exist for runup height, aiming at a quick estimate of the tsunami-induced coastal inundation (e.g., Madsen and Schaeffer (2010); Park et al. (2015)).

To scale the inputs of the procedure from basin-level down to local coasts, a modeling chain concept is applied, as already done in several coastal applications with good results (Federico et al., 2017; Gaeta et al., 2018; Postacchini et al., 2019; Postacchini & Ludeno, 2019). Practical examples of the methodology are finally given for selected coastal areas (Esaro river estuary, Calabria, and Bari, Apulia) exposed to tsunami waves approaching perpendicularly and obliquely, respectively. The method is application-oriented and is meant to support stakeholders and coastal managers as a tool for the evaluation of tsunami risk potential.

The modeling chain and the proposed semi-analytical approach are described in Section 2. Results are given in Section 3 and discussed in Section 4, along with concluding remarks.

2. Methods

2.1. Modeling Chain

A conceptual map of the modeling chain is given in Figure 1. The first step of the procedure is tackled with a realistic approach: a tsunami wave is generated at a hypothetical earthquake epicenter located in the Hellenic arc, notoriously the most seismically active region of the Mediterranean Sea (Figure 2). The initial surface displacement then propagates across the basin in a *large-scale modeling*, to infer realistic tsunami front directions at intermediate depths in front of the coasts of interest. An extraction depth of 50 m has been chosen in this application.

In the second step, a set of numerical simulations is run (*intermediate-scale modeling*), in which tsunami-like waves are propagated from intermediate waters to the nearshore region in front of the southern Italian coasts (Apulia, Basilicata, Calabria, Sicily; orange outline in Figure 2), which are the most prone to inundation from tsunami waves generated in the Hellenic arc (Maramai et al., 2021). The purpose of intermediate-scale modeling is to gather an along-coast distribution of a parameter named α, devised to serve as a proxy for the several processes (e.g., shoaling, refraction, diffraction) that the modeled tsunami, given a propagating direction derived from the previous large-scale modeling, will undergo during its propagation from intermediate to shallow waters. Since α is clearly dependent on the direction of the approaching tsunami front, distributions of α have been evaluated for two significant conditions. Besides evaluating α from realistic tsunami directions inferred from the previous large-scale modeling, also α from perpendicularly approaching tsunami fronts have been considered as an extreme, largely conservative case in which dissipation from refraction is minimal under the hypothesis of very long waves.

After the parameter distributions are obtained, values of α are used in the third step as a "scaling factor" to transport the properties of the tsunami wave from intermediate depths (i.e., the wave used as input for intermediate-scale modeling) up to shallow waters, as described in Section 2.4. The so-scaled wave, which is now assumed to have undergone all the transformation processes represented by α whether for a conservative or a realistic approach, is used as an initial condition for a *small-scale modeling* to finally get an estimate of coastal inundation.

2.2. The Analytical Solution: Green's Law Generalization

Lalli et al. (2019) have proposed a semi-analytical approach to characterize the transformation process of tsunami-like long waves over general bathymetries: the approach involves a generalization of Green's law (Dean & Dalrymple, 1991) with a generalizing parameter α:

$$H_1 = \alpha\, H_0 \left(\frac{d_0}{d_1}\right)^{1/4} \tag{1}$$

where H_0 and d_0 are the wave height and depth at an offshore location (or in deep water), and H_1 and d_1 are the respective values at a location closer to the shore. α is to be evaluated empirically with the use of suitable numerical simulations of long wave propagation over the complex bathymetry of interest. α is calculated as

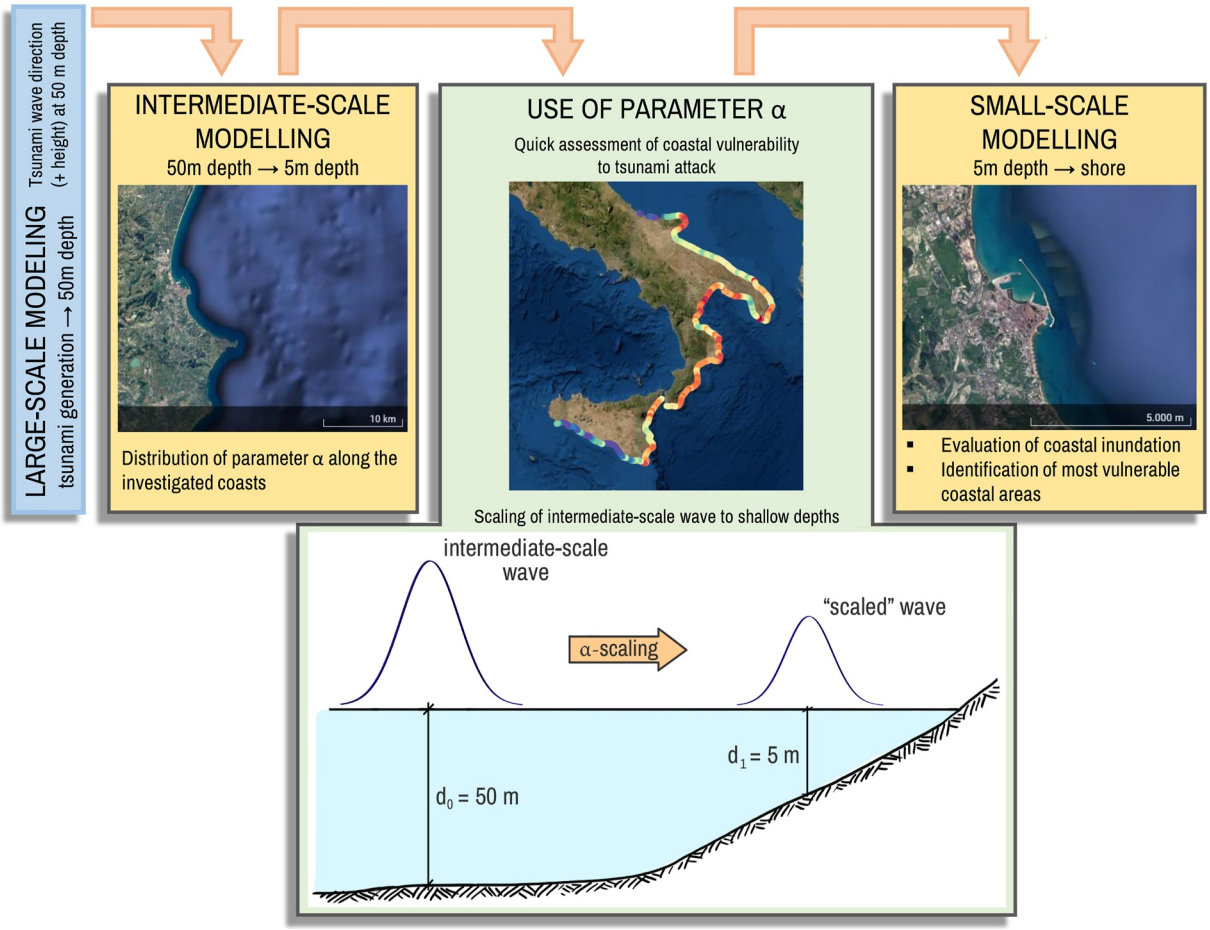

Figure 1. Conceptual scheme of the modeling chain.

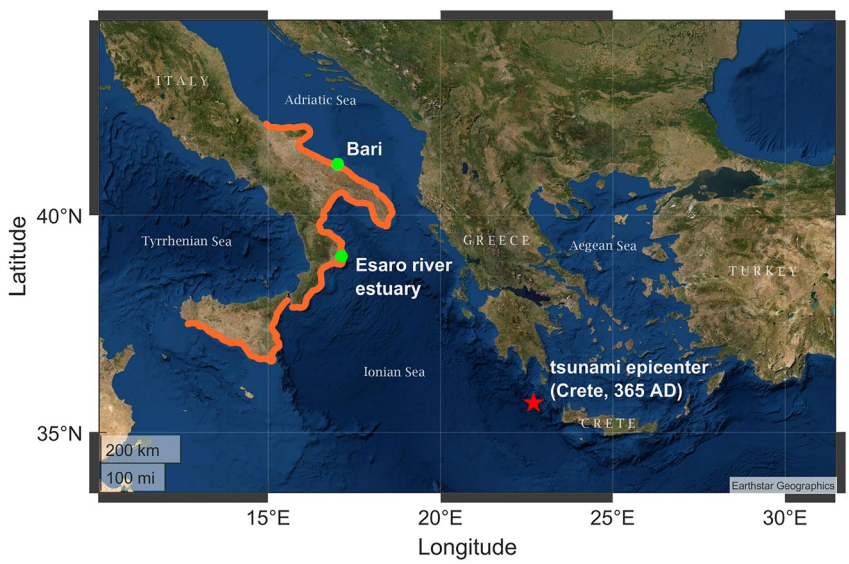

Figure 2. Map of the central Mediterranean Sea. The Italian coasts chosen for the evaluation of α (orange outline), location of the Esaro river estuary and Bari (green circles) and the epicenter of the prototype tsunami event (red star; Stiros (2001)) are shown.

$$\alpha = \sqrt{\frac{\tilde{\Phi}_1}{\tilde{\Phi}_0}} \tag{2}$$

where $\tilde{\Phi}_1$ is the time-cumulative energy flux of the long wave evaluated at any given depth d_1, and $\tilde{\Phi}_0$ is the flux at an offshore location d_0. α can be considered as a proxy of how much the tsunami energy flux changes as it travels from the deep sea to shallow waters, by virtue of processes other than pure shoaling. The linear approximation of the specific energy flux is

$$\Phi = g d \eta |V| \tag{3}$$

where η is the surface elevation, d is the undisturbed water depth, and V is the depth-averaged fluid velocity.

In a sense, α is similar in concept to the classical refraction coefficient adopted to model the change in wave height due to refraction. However, it assumes a much broader meaning when evaluated by numerical modeling, as it also encompasses every contribution to long waves transformation other than shoaling, for example, reflection, diffraction and other interactions with natural obstacles and artificial structures.

2.3. The Shallow-Water Model

The α parameter of Equation 2 is numerically evaluated with flux data from numerical simulations of long wave propagation at an intermediate-scale. Simulations are performed using the model SASHA (Staggered ANPA SHallow wAter; Lalli et al. (2001); Lalli et al. (2010)), which solves the shallow water equations with a finite difference scheme deployed on a staggered Cartesian grid. Such equations represent the conservation of mass and momentum:

$$\frac{\partial \eta}{\partial t} + \frac{\partial U}{\partial x} + \frac{\partial V}{\partial y} = 0, \tag{4}$$

$$\frac{\partial U}{\partial t} + \frac{\partial \left(U^2/h\right)}{\partial x} + \frac{\partial (UV/h)}{\partial y} = = -gh\frac{\partial \eta}{\partial x} + 2\frac{\partial}{\partial x}\left(\mu h \frac{\partial u}{\partial x}\right) + \frac{\partial}{\partial y}\left[\mu h\left(\frac{\partial v}{\partial x} + \frac{\partial u}{\partial y}\right)\right] - F_u U, \tag{5}$$

$$\frac{\partial V}{\partial t} + \frac{\partial (UV/h)}{\partial x} + \frac{\partial \left(V^2/h\right)}{\partial y} = = -gh\frac{\partial \eta}{\partial y} + 2\frac{\partial}{\partial y}\left(\mu h \frac{\partial v}{\partial y}\right) + \frac{\partial}{\partial x}\left[\mu h\left(\frac{\partial v}{\partial x} + \frac{\partial u}{\partial y}\right)\right] - F_v V. \tag{6}$$

The term μ, assumed constant, includes both molecular and eddy viscosity components; F_u and F_v represent friction factors. u and v are depth-averaged horizontal velocities in the x and y directions; h is the total water depth and $U = hu$, $V = hv$. Finally, the total local water depth is approximated with the undisturbed depth ($h \approx d$), so that $U \approx hu$ and $V \approx hv$. Further details and applications can be found in Lalli et al. (2001, 2010, 2019).

Intermediate-scale simulations in SASHA have been performed for each subdomain into which the southern Italy coastlines has been divided into (Figures 5a and 5b). An absorbing layer, whose length is equal to half the length of the input prototype wave, has been placed at the landward edge of the modeled region to dissipate the residual wave energy once the long wave has trespassed the 5 m depth isobath. Sponge layers have also been placed at the seaward and lateral sides of the domain to absorb spurious reflected waves.

On the basis of preliminary tests, input waves have been set up at the offshore boundary of each domain and then propagated between 50-m and 5-m depths, bearing in mind that SASHA is implemented in linearized form in the present work and its results are independent of the wave height imposed at the offshore boundary (Lalli et al., 2019). The nearshore cumulative energy flux $\tilde{\Phi}_1$ is estimated with Equation 3 after the whole wave has traveled through the 5 m isobath, assumed as the closure depth of the beach, and finally used to evaluate α by means of Equation 2.

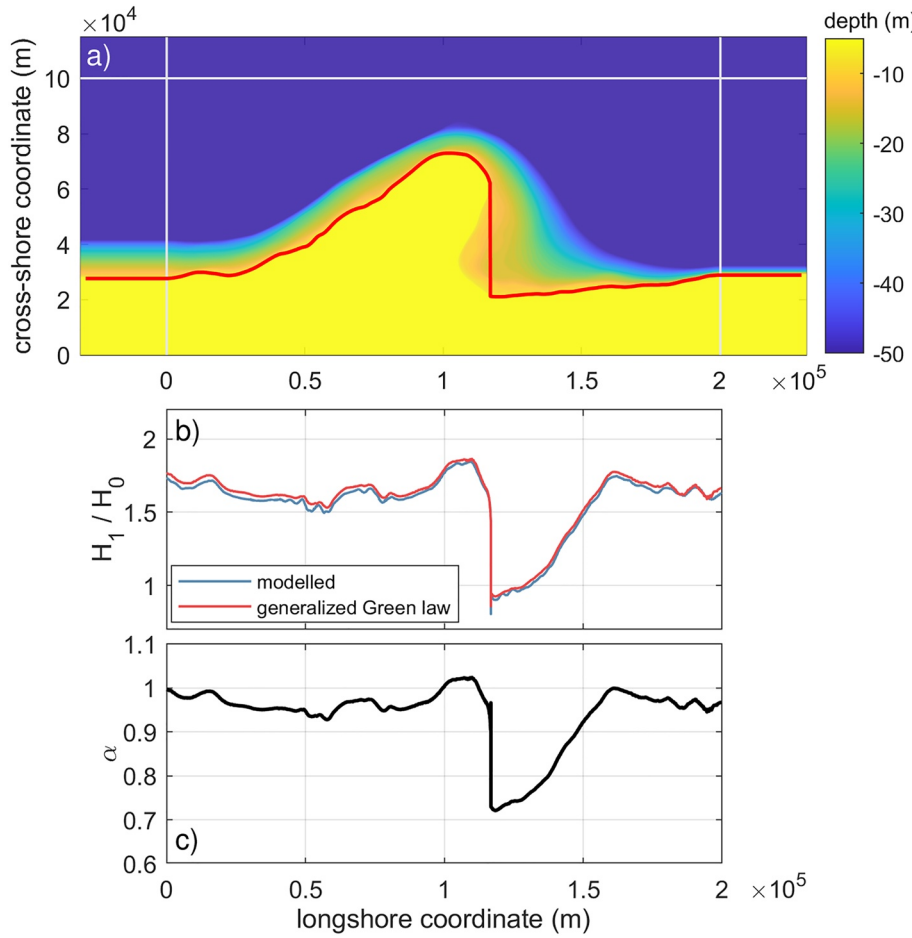

Figure 3. Configuration and output of a typical intermediate-scale simulation with SASHA; (a) numerical domain. The 5-m isobath (red line) and the limits of the sponge layers (gray lines) are shown; (b) H_1/H_0 at the 5 m isobath, modeled by SASHA (blue line) and evaluated with Equation 1 (red line); (c) distribution of modeled α along the 5-m isobath.

An example of the setting and output of a typical intermediate-scale simulation with SASHA is given in Figure 3 for the Gargano headland (Apulia) for a prototype wave approaching perpendicularly to shore. Figure 3a shows the bathymetry over which the input wave propagates and the 5-m isobath at which the energy flux is calculated (red line). Figure 3b shows the ratio H_1/H_0 as directly modeled by SASHA (blue line) and as evaluated semi-analytically with the generalized Green's law (red line). A good correspondence of the two curves gives confidence in the method. Values of α along the 5-m isobath are given in Figure 3c.

2.4. Methodology for the Assessment of Flooding

The distribution of α along any given coast is employed to "scale" the tsunami wave properties, that is, to evaluate its height and length in shallow waters (depth $d_1 = 5$ m), once the height at intermediate depth ($d_0 = 50$ m) is known. A conceptual scheme of the scaling process to move intermediate-scale wave input toward shallow depths is given in the bottom panel of Figure 1.

The shallow-water wave height H_1 is first calculated by Equation 1, with α taken as the mean value $\overline{\alpha}$ along the coastal stretch being investigated:

$$H_1 = \overline{\alpha}\, H_0 \left(\frac{d_0}{d_1}\right)^{1/4}. \tag{7}$$

Under the commonly assumed hypothesis that the wave period is conserved between d_0 and d_1, the shallow water wave length L_1 is calculated by the definition of the solitary wavenumber provided in Madsen et al. (2008):

$$L_1 = \frac{2\pi}{k_1} = 4\pi d_0 \sqrt{\frac{d_1}{3H_0}} \tag{8}$$

where k_1 is the wavenumber of the solitary wave in shallow waters. L_1 is therefore taken as the tsunami wavelength at depth d_1. A solitary wave characterized by wave height H_1 and length L_1 is finally applied as initial condition at depth d_1, to be used for the shallow-water simulation for the evaluation of shoreline motion and coastal inundation.

3. Results

3.1. Large-Scale Modeling: Tsunami Propagation in the Mediterranean Sea

One of the most catastrophic seismic events in the history of the Mediterranean Sea occurred in 365 A.D (Stiros, 2001), with epicenter to the West of Crete island, in the Hellenic arc (the red star in Figure 2). A simple numerical recreation of this tsunami is considered in our application, to evaluate the global impact of a typical tsunami on southern Italian coasts and estimate the main approach direction of the long wavefront. Although the main focus of our work is to define a semi-empirical procedure based on a linear solver and illustrate its application, a preliminary modeling with the renowned nonlinear solver FUNWAVE-TVD (Shi et al., 2012) is made on a basin level.

In line with other works (e.g., Molinari et al. (2016); Gibbons et al. (2020)), a Gaussian hump has been used to model a prototype tsunami originating in the west Hellenic arc. The hump has a maximum height of 5 m, while its major axis has an orientation of 45°N to follow the direction of the local underwater fault. These simple shape and orientation have been chosen for applicative purposes; other solutions for seabed or surface initial displacements, like those by Mansinha and Smylie (1971) and Okada (1985), are valid albeit more complex alternatives. The numerical grid covering the central part of the Mediterranean Sea has been built using bathymetric data available at the online platform GEBCO (Weatherall et al., 2015).

Figure 4 illustrates the maximum modeled water elevation in the central Mediterranean Sea. The output of such typical scenario is used to identify the propagation direction of the tsunami wave in front of the coasts of interest, at 50-m water depth, that is, the offshore location where intermediate-scale modeling is initiated. Figure 4 shows that portions of the Apulian and Sicilian coasts experience the most angled waves, that is, respectively, inclined of ∼60° with respect to the direction orthogonal to the coast and almost parallel to the coast (Figures 4a and 4b).

3.2. Intermediate-Scale Modeling: α Distribution Along the Southern Italian Coasts

The parameter α has been computed along the Italian coasts by subdividing the interested coastlines into a number of domains of variable cross-shore and longshore sizes, generally in the order of 100–200 km and grid size of 150 m. The bathymetries have been smoothed with a median filter to remove spikes and ensure a smooth wave transformation. Two different approaches have been used to evaluate α: (a) the *realistic* case, for which the tsunami directions are inferred from the previous large-scale modeling, and (b) the *conservative* case, for which the tsunami always approaches perpendicularly to the coast.

Figures 5a and 5b shows the domains used to evaluate α in the case of realistic tsunami fronts inferred from basin-scale modeling. The α distribution along the investigated coasts is given in Figures 5c and 5e for realistic tsunami waves. The values of α have been evaluated from the outcome of intermediate-scale simulations with SASHA: small and high values of α are indicative of low tsunami impact (small residual energy flux at 5 m depth) and high tsunami impact (high residual energy flux at 5 m depth), respectively.

The smallest values of α are observed in areas that are less exposed to the action of a tsunami approaching at a realistic angle, due to their favorable geographical location. The coast north of the Apulia Region (Figure 5c) is characterized by small values of α (<0.4), as it is protected by the Gargano Promontory, which is in turn much more susceptible to tsunami energy ($\alpha > 1$). A similar behavior is observed in Sicily (Figure 5e), whose southern and western coasts ($\alpha < 0.4$) are more protected than the eastern coasts ($\alpha \approx 1$). The whole Calabria coast is

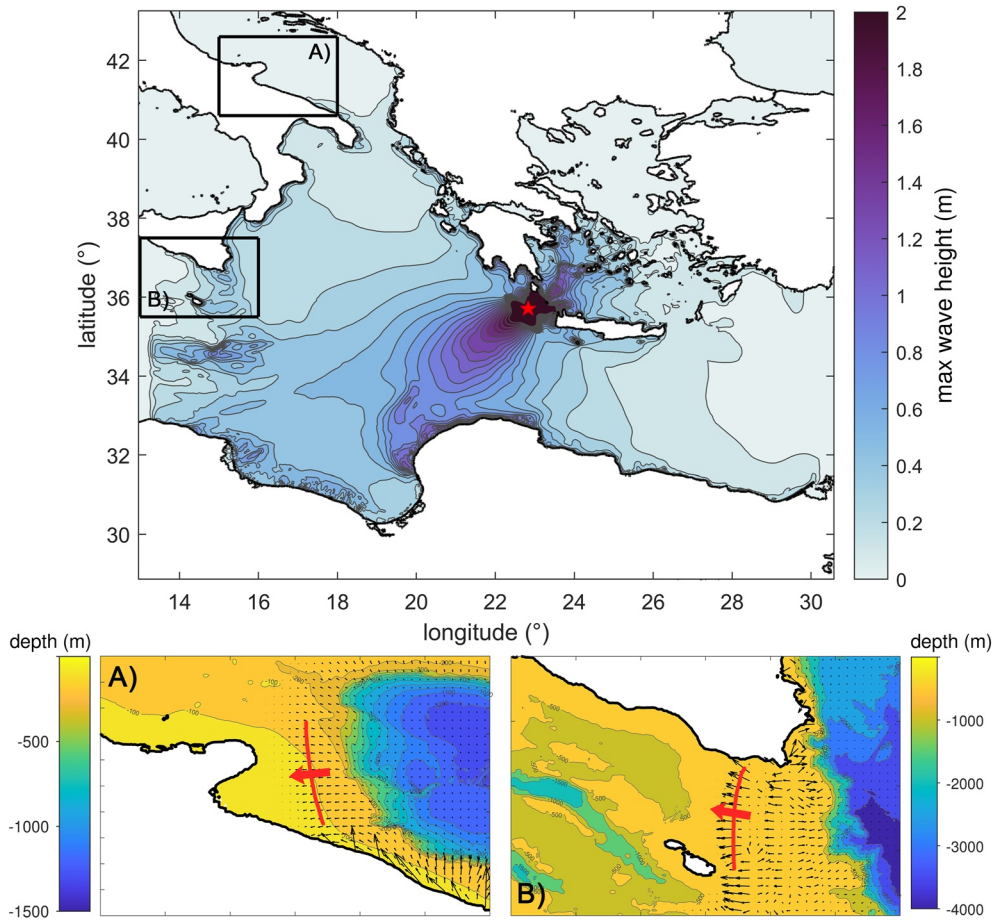

Figure 4. Map of the maximum water level modeled by FUNWAVE-TVD for a prototype tsunami originated from the Hellenic arc, west of Crete Island (red star). The modeled directions of approach of the tsunami wavefront (red lines and arrows) for Apulia and southern Sicily are highlighted in panels (a and b). Black vectors represent the modeled tsunami wave velocity fields.

highly impacted by the tsunami wave, with $\alpha \approx$ (0.8–1) almost everywhere and the most exposed area being the Taranto Gulf. Less impacted is the Adriatic Apulia coast, with $\alpha \approx$ (0.5–0.6) on average, while the southernmost part of Apulia is highly exposed ($\alpha \approx 1$).

The same distributions of α for the conservative case (normal-to-coast tsunamis) are shown in Figures 5d and 5f. Such conservative scenario differs the most from that with realistic tsunami wave approach (Figures 5c and 5e) in the Sicilian and Apulian coasts. The latter ones are the mostly exposed to the hazard of normal-to-coast tsunamis, with $\alpha \approx$ (0.9–1) and above. This is due to the wide, gentle bathymetric slopes in front of the Apulian shores, which lead to enhanced shoaling when the tsunami approaches perpendicularly, in contrast to the more irregular seabed configuration in front of southern Sicily (Figures 4a and 4b).

3.3. Small-Scale Modeling: Nearshore Propagation and Flooding

As illustrative examples, α from the intermediate-scale modeling campaign with realistic and normal-to-coast input waves are exploited to model flooding levels in two regions of southern Italy: the Esaro river estuary (Calabria) and Bari (Apulia). The chosen locations are characterized by urbanized settings with industrial, residential and recreational areas, and are thus representative of typical Italian coastal environments. Due to the geographical location of the Esaro River estuary (Figure 2), tsunami waves mainly approach the coast perpendicularly, and the small-scale modeling may be thus applied using the conservative case. On the other hand,

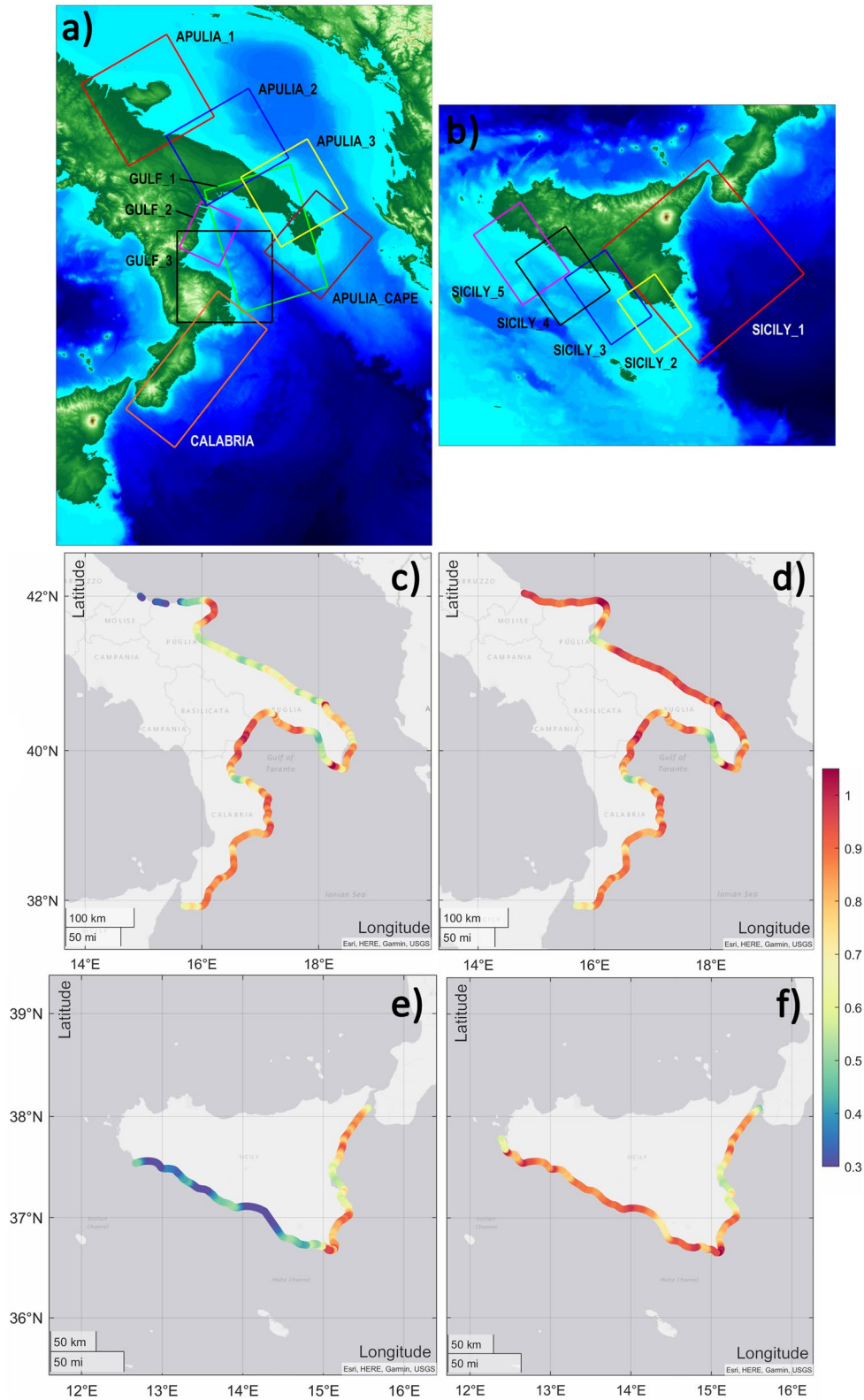

Figure 5. (a and b) Domains used for the SASHA simulation campaign in the realistic case; (c and e) distribution of α evaluated for the realistic case; (d and f) distribution of α evaluated for the conservative case (perpendicular tsunami fronts).

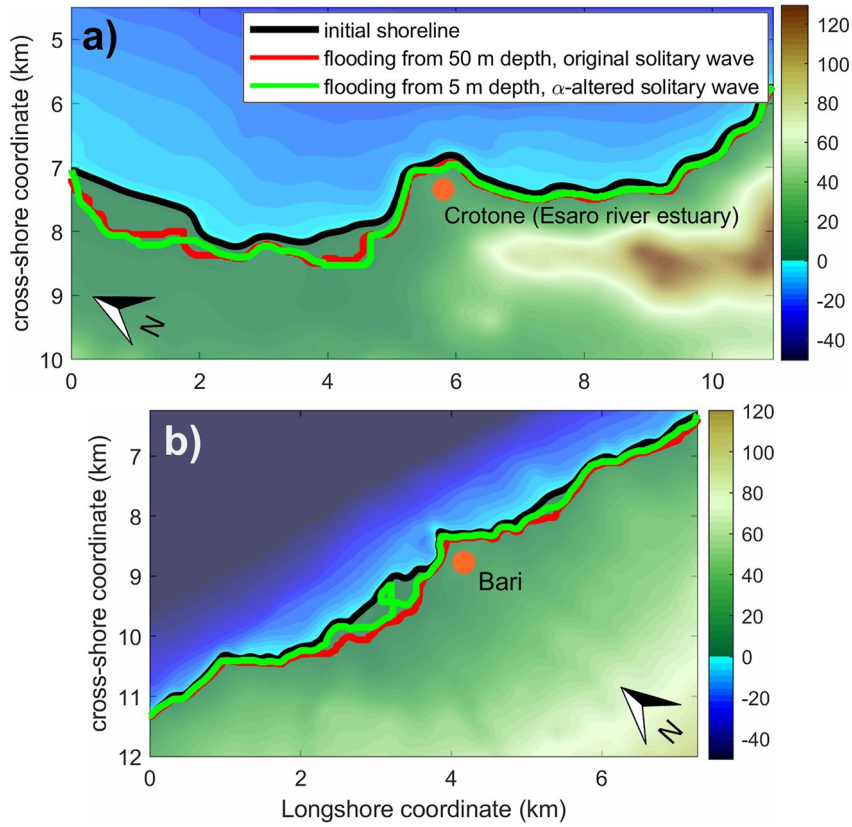

Figure 6. Coastal areas (a) around the Esaro River estuary, and (b) around Bari used as numerical domains for the small-scale modeling, and comparison of shorelines simulated with the tested approaches: initial shoreline (black line), maximum inundation of a 2-m solitary wave at a 50-m depth (red line), maximum inundation of the α-scaled solitary wave imposed at 5-m depth (green line).

the Bari coastline is approached by the prototype tsunami in an oblique fashion (Figure 4a) and is thus taken as representative of the application of α from the realistic case.

Shallow-water, small-scale coastal modeling is performed using FUNWAVE-TVD on computational domains with a maximum offshore depth of 5 m (i.e., the depth at which α is evaluated). The definition of wave input for these simulations implements the concept of α as a proxy of seabed-induced effects; that is, the wave form used as input for intermediate-scale modeling (50 m) is "scaled" through α to reduce it at 5-m depth. The "scaled" wave input is then applied as an initial condition of water surface displacement at a water depth 5 m and used to evaluate coastal flooding. The scaling is performed with the formulas given in Section 2.4. With the use of α, all bathymetry-related dynamics influencing the solitary wave height (shoaling, refraction, diffraction) are included when transporting wave data from intermediate to shallow waters. This application allows us to show that a good representation of tsunami-induced inundation can also be achieved with input data from simpler, linear tools and semi-analytical concepts.

We assume that the tsunami height at $d_0 = 50$ m is $H_0 = 2$ m. Provided that the mean values of α are 0.853 for the Esaro case and 0.59 for the Bari case, the "scaled" input waves to be imposed at $d_1 = 5$ m depth would have a wave height $H_1 = 3.03$ m for the Esaro case and 2.13 m for the Bari case. The wavelength is $L_1 = 573.57$ m for both cases.

We make a comparison of coastal flooding levels obtained with the two previously mentioned approaches: (a) intermediate-scale simulation on a 25×25 m grid with a 2-m solitary wave at offshore depth 50 m, and (b) small-scale simulations on a 15×15 m grid with the "scaled" waves at offshore depth 5 m. Figure 6 shows maximum shoreline motions for both approaches in the two tests. The modeled shorelines are overall in good agreement, although some discrepancies are seen in the flattest regions of the investigated coasts. This lends support to a

fruitful use of α as a tool to move modeling efforts toward smaller scales once offshore tsunami data are known, by either observation or previous modeling. In these applications, the small-scale simulations achieved a reduction of about 41% in computational time with respect to intermediate-scale simulations.

4. Discussion and Conclusions

The method here proposed can be profitably used from an operational point of view, by end-level users in the field of coastal protection and structure design. The parameter α can serve as support for coastal design and decision making by allowing for varying levels of prudence. α established with normal-to-coast fronts can be assumed as "universal", conservative values pertaining to the capability of a given seabed configuration to alter the potentiel tsunami hazard, since the front direction does not enter as a variable and only bathymetry-related effects are accounted for. This approach is particularly useful when deep sea tsunami information is scarce or unreliable, or when the evaluation of the general protection capacity of a coastal stretch is of interest. Conversely, when specific, low-cost protection strategies are required, α evaluated with a realistic wave angle allows one to account for the effects of both tsunami direction and bathymetry. Use of oblique wave fronts is also desirable for studies involving indented coasts, where effects of wave sheltering and complex refraction might be important. In coasts where differences in α pertaining to normal-to-coast versus realistic tsunami fronts are relevant (like the Adriatic coasts of Apulia and the southern coasts of Sicily), values of α from both approaches might be considered to account for different levels of design safety.

The proposed applications, moreover, show that once α is available in a specific coastal area, inundation can be evaluated by running only a small-scale simulation over the coast of interest, while pre-defined information (e.g., wave direction and α) are known beforehand to speed up the whole forecasting process. The method allows for the down-scaling of the computational effort toward the small regional scales once information from a relatively coarser basin-scale simulation is available. This favors a fast (order of a few minutes) yet reliable deterministic first estimates of tsunami impact (Selva et al., 2021). A reliable estimate will also reduce underestimation of tsunami impact and fatal missed alarms, as occurred during the 2011 Tohoku tsunami event (Makinoshima et al., 2021).

Although the effect on the runup of different tsunami-wave forms is worth of investigation (e.g., Madsen et al. (2008); Madsen and Schaeffer (2010)), we have chosen a solitary shape both for simplicity sake and for its use in empirical runup models (Park et al., 2015) and in early warning systems when the tsunami wave shape is unknown (Didenkulova et al., 2008).

The modeling chain has its starting point in the definition of a prototypical tsunami based on a real, catastrophic event: in the framework of tsunami risk assessment models, the procedure proposed here is thus similar to a worst-case plausible scenario. The analysis of a limited number or even single scenarios, as performed in our work, may be put in tandem with previous probabilistic hazard assessments (like those described in Tonini et al. (2021) and Selva et al. (2021)) in the perspective of narrowing tsunami variability down to a range of most probable parameters.

Fundamental to the semi-empirical implementation of the Green's law given here is the explicit consideration of the effects of bathymetry over the deformation of the wavefront and, eventually, over tsunami impact. Bathymetry effects are inherently neglected in non-probabilistic procedures for tsunami-related alert states like decision matrices (Selva et al., 2021), and circumvented by end-to-end forecasting methods like neural networking (Makinoshima et al., 2021). On the other hand, probabilistic methods deal with the unknown effects of bathymetry only with varying uncertainty bounds on forecast results (Selva et al., 2021).

We aim at improving the methodology further by tackling other sources of uncertainty, like fault orientation and the subsequent main direction of propagation (Selva et al., 2021).

Data Availability Statement

A data set including input and output data for the presented simulations is available at the Zenodo repository referenced in Melito et al. (2022). Version 3.6 of the software FUNWAVE-TVD has been used for hydrodynamic modeling; the model is in the public domain and can be downloaded at the following page: https://github.com/

fengyanshi/FUNWAVE-TVD/releases/tag/Version_3.6. bathymetries are freely available at the GEBCO platform: https://www.gebco.net.

Acknowledgments
The study is funded by Circeo National Park and Gargano National Park within the National Biodiversity Strategy promoted by the Ministero dell'Ambiente e della Tutela del Territorio e del Mare (MATTM), Italy (GAB0024444). Support from the Office of Naval Research Global (UK) MORSE Project (Research Grant No. N62909-17-1-2148), the MIUR PRIN 2017 Project "FUNdamentals of BREAKing wave-induced boundary dynamics—FUNBREAK" (Grant No. 20172B7MY9), and the Italian Civil Protection in the framework of the Italian Tsunami Directive is gratefully acknowledged. The authors would like to thank the two anonymous reviewers, whose comments improved the quality of the manuscript. Open Access Funding provided by Universita Politecnica delle Marche within the CRUI-CARE Agreement.

References

Ambraseys, N., & Synolakis, C. (2010). Tsunami catalogs for the Eastern Mediterranean, revisited. *Journal of Earthquake Engineering*, *14*(3), 309–330. https://doi.org/10.1080/13632460903277593

Anfuso, G., Postacchini, M., Di Luccio, D., & Benassai, G. (2021). Coastal sensitivity/vulnerability characterization and adaptation strategies: A review. *Journal of Marine Science and Engineering*, *9*(1), 72. https://doi.org/10.3390/jmse9010072

Bonaldo, D., Antonioli, F., Archetti, R., Bezzi, A., Correggiari, A., Davolio, S., et al. (2019). Integrating multidisciplinary instruments for assessing coastal vulnerability to erosion and sea level rise: Lessons and challenges from the Adriatic Sea, Italy. *Journal of Coastal Conservation*, *23*(1), 19–37. https://doi.org/10.1007/s11852-018-0633-x

Chaib, W., Guerfi, M., & Hemdane, Y. (2020). Evaluation of coastal vulnerability and exposure to erosion and submersion risks in Bou Ismail Bay (Algeria) using the coastal risk index (CRI). *Arabian Journal of Geosciences*, *13*(11), 1–18. https://doi.org/10.1007/s12517-020-05407-6

Choi, B., Kaistrenko, V., Kim, K., Min, B., & Pelinovsky, E. (2011). Rapid forecasting of tsunami runup heights from 2-d numerical simulations. *Natural Hazards and Earth System Sciences*, *11*(3), 707–714. https://doi.org/10.5194/nhess-11-707-2011

Da Lio, C., & Tosi, L. (2019). Vulnerability to relative sea-level rise in the Po river delta (Italy). *Estuarine, Coastal and Shelf Science*, *228*, 106379. https://doi.org/10.1016/j.ecss.2019.106379

Dean, R. G., & Dalrymple, R. A. (1991). *Water Wave Mechanics for Engineers and Scientists* (Vol. 2). World Scientific. https://doi.org/10.1142/1232

Didenkulova, I., Pelinovsky, E., & Soomere, T. (2008). Runup characteristics of symmetrical solitary tsunami waves of "unknown" shapes. *Pure and Applied Geophysics*, *165*(11), 2249–2264. https://doi.org/10.1007/s00024-008-0425-6

Federico, I., Pinardi, N., Coppini, G., Oddo, P., Lecci, R., & Mossa, M. (2017). Coastal ocean forecasting with an unstructured grid model in the southern Adriatic and northern Ionian seas. *Natural Hazards and Earth System Sciences*, *17*(1), 45–59. https://doi.org/10.5194/nhess-17-45-2017

Gaeta, M. G., Bonaldo, D., Samaras, A. G., Carniel, S., & Archetti, R. (2018). Coupled wave-2D hydrodynamics modeling at the Reno river mouth (Italy) under climate change scenarios. *Water*, *10*(10), 1380. https://doi.org/10.3390/w10101380

Gibbons, S. J., Lorito, S., Macías, J., Løvholt, F., Selva, J., Volpe, M., et al. (2020). Probabilistic tsunami hazard analysis: High performance computing for massive scale inundation simulations. *Frontiers of Earth Science*, *8*, 623. https://doi.org/10.3389/feart.2020.591549

Hzami, A., Heggy, E., Amrouni, O., Mahé, G., Maanan, M., & Abdeljaouad, S. (2021). Alarming coastal vulnerability of the deltaic and sandy beaches of North Africa. *Scientific Reports*, *11*(1), 1–15. https://doi.org/10.1038/s41598-020-77926-x

Lalli, F., Berti, D., Miozzi, M., Miscione, F., Porfidia, B., Serva, L., et al. (2001). Analysis of breakwater-induced environmental effects at Pescara (Adriatic Sea, Italy) channel-harbor. In *The eleventh international offshore and polar engineering conference*.

Lalli, F., Bruschi, A., Lama, R., Liberti, L., Mandrone, S., & Pesarino, V. (2010). Coanda effect in coastal flows. *Coastal Engineering*, *57*(3), 278–289. https://doi.org/10.1016/j.coastaleng.2009.10.015

Lalli, F., Postacchini, M., & Brocchini, M. (2019). Long waves approaching the coast: Green's law generalization. *Journal of Ocean Engineering and Marine Energy*, *5*(4), 385–402. https://doi.org/10.1007/s40722-019-00152-9

Lay, T., Kanamori, H., Ammon, C. J., Nettles, M., Ward, S. N., Aster, R. C., et al. (2005). The great Sumatra-Andaman earthquake of 26 December 2004. *Science*, *308*(5725), 1127–1133. https://doi.org/10.1126/science.1112250

Madsen, P. A., Fuhrman, D. R., & Schäffer, H. A. (2008). On the solitary wave paradigm for tsunamis. *Journal of Geophysical Research*, *113*(C12). https://doi.org/10.1029/2008jc004932

Madsen, P. A., & Schaeffer, H. A. (2010). Analytical solutions for tsunami runup on a plane beach: Single waves, N-waves and transient waves. *Journal of Fluid Mechanics*, *645*, 27–57. https://doi.org/10.1017/s0022112009992485

Makinoshima, F., Oishi, Y., Yamazaki, T., Furumura, T., & Imamura, F. (2021). Early forecasting of tsunami inundation from tsunami and geodetic observation data with convolutional neural networks. *Nature Communications*, *12*(1), 1–10. https://doi.org/10.1038/s41467-021-22348-0

Mansinha, L., & Smylie, D. E. (1971). The displacement fields of inclined faults. *Bulletin of the Seismological Society of America*, *61*(5), 1433–1440. https://doi.org/10.1785/bssa0610051433

Maramai, A., Brizuela, B., & Graziani, L. (2014). The Euro-Mediterranean tsunami catalogue. *Annals of Geophysics-Italy*, *57*(4). https://doi.org/10.4401/ag-6437

Maramai, A., Graziani, L., & Brizuela, B. (2021). Italian Tsunami Effects Database (ITED): The first database of tsunami effects observed along the Italian coasts. *Frontiers of Earth Science*, *9*, 137. https://doi.org/10.3389/feart.2021.596044

Melito, L., Lalli, F., Postacchini, M., & Brocchini, M. (2022). Simulation data for a semi-empirical approach for tsunami inundation in South Italy [dataset]. Zenodo. https://doi.org/10.5281/zenodo.6249936 .

Molinari, I., Tonini, R., Lorito, S., Piatanesi, A., Romano, F., Melini, D., et al. (2016). Fast evaluation of tsunami scenarios: Uncertainty assessment for a Mediterranean Sea database. *Natural Hazards and Earth System Sciences*, *16*(12), 2593–2602. https://doi.org/10.5194/nhess-16-2593-2016

Mori, N., Takahashi, T., Yasuda, T., & Yanagisawa, H. (2011). Survey of 2011 Tohoku earthquake tsunami inundation and run-up. *Geophysical Research Letters*, *38*(7). https://doi.org/10.1029/2011gl049210

Okada, Y. (1985). Surface deformation due to shear and tensile faults in a half-space. *Bulletin of the Seismological Society of America*, *75*(4), 1135–1154. https://doi.org/10.1785/BSSA0750041135

Park, H., Cox, D. T., & Petroff, C. M. (2015). An empirical solution for tsunami run-up on compound slopes. *Natural Hazards*, *76*(3), 1727–1743. https://doi.org/10.1007/s11069-014-1568-7

Postacchini, M., Lalli, F., Memmola, F., Bruschi, A., Bellafiore, D., Lisi, I., et al. (2019). A model chain approach for coastal inundation: Application to the bay of Alghero. *Estuarine, Coastal and Shelf Science*, *219*, 56–70. https://doi.org/10.1016/j.ecss.2019.01.013

Postacchini, M., & Ludeno, G. (2019). Combining numerical simulations and normalized scalar product strategy: A new tool for predicting beach inundation. *Journal of Marine Science and Engineering*, *7*(9), 325. https://doi.org/10.3390/jmse7090325

Satake, K. (1988). Effects of bathymetry on tsunami propagation: Application of ray tracing to tsunamis. *Pure and Applied Geophysics*, *126*(1), 27–36. https://doi.org/10.1007/bf00876912

Selva, J., Lorito, S., Volpe, M., Romano, F., Tonini, R., Perfetti, P., et al. (2021). Probabilistic tsunami forecasting for early warning. *Nature Communications*, *12*(1), 1–14. https://doi.org/10.1038/s41467-021-25815-w

Shi, F., Kirby, J. T., Harris, J. C., Geiman, J. D., & Grilli, S. T. (2012). A high-order adaptive time-stepping TVD solver for Boussinesq modeling of breaking waves and coastal inundation. *Ocean Modelling*, *43*, 36–51. https://doi.org/10.1016/j.ocemod.2011.12.004

Stiros, S. C. (2001). The AD 365 Crete earthquake and possible seismic clustering during the fourth to sixth centuries AD in the eastern mediterranean: A review of historical and archaeological data. *Journal of Structural Geology*, *23*(2–3), 545–562. https://doi.org/10.1016/s0191-8141(00)00118-8

Tonini, R., Di Manna, P., Lorito, S., Selva, J., Volpe, M., Romano, F., et al. (2021). Testing tsunami inundation maps for evacuation planning in Italy. *Frontiers of Earth Science*, *9*. https://doi.org/10.3389/feart.2021.628061

Weatherall, P., Marks, K. M., Jakobsson, M., Schmitt, T., Tani, S., Arndt, J. E., et al. (2015). A new digital bathymetric model of the world's oceans. *Earth and Space Science*, *2*(8), 331–345. https://doi.org/10.1002/2015ea000107